

# A perspective shape-from-shading method using fast sweeping numerical scheme

YANG LEI<sup>1\*</sup>, HAN JIU-QIANG<sup>2</sup>

<sup>1</sup>School of Economics and Management, Tongji University, Shanghai 200092, China

<sup>2</sup>School of Electronics and Information Engineering, Xi'an Jiaotong University, Xi'an 710049, China

\*Corresponding author: yangyoungya@sina.com

Shape-from-shading (SFS) is an approach of 3-D shape reconstruction from only one image. A new perspective SFS method is proposed in this paper. Firstly, a reflectance map equation under perspective projection is introduced. Then, the reflectance map equation turns into a static Hamilton–Jacobi equation. So the SFS problem is formulated as a viscosity solution of the static Hamilton–Jacobi equation. The fast sweeping numerical method is used to solve the Hamilton–Jacobi equation and a new SFS method is gained. At last, experiments on both synthetic and real images are given. Experiments on the synthetic image show that the proposed SFS method is fast and accurate. Results of the real image show the efficiency of the proposed method when dealing with complicated real surface, and new criteria to evaluate the performance of the method are proposed.

Keywords: shape-from-shading, reflectance map, viscosity solution, Hamilton–Jacobi equation, perspective projection.

## 1. Introduction

Shape-from-shading (SFS) is an approach of 3-D shape reconstruction from only one image, which is a classical 3-D measure method in computer vision [1]. SFS reconstructs the 3-D shape of a surface based on the reflectance map equation satisfied by each pixel point of image [2]. The development of SFS mainly depends on two aspects, the search for suitable reflectance models and the investigation into the effective SFS algorithms [3]. The original SFS algorithm was based on the principle of variations [2]. SFS is widely applied in industry inspection, terrain analysis such as the moon or oceans [4–6], and so on.

The first SFS method was proposed by Horn in the early 1970s [1]. This approach was based on minimizing the total error function consisting of one or several constraints such as brightness, smoothness, and so on. After the SFS problem was proposed, different new computational techniques have been introduced into SFS by

both computer vision and mathematical workers. Zhang classified the traditional SFS computational approach into four categories [2]. Neural networks methods have also been recently employed [3, 7]. Lately, a statistical approach has been proposed [8]. 3-D SFS reconstruction based on a more general, varying reflectance model was proposed in 2005 [9]. Among these methods, a partial differential equations (PDEs) based SFS method is an important kind of a reconstruction method. Characteristics-lines method in [1] is the earliest one. And an optimal control theory can be used to solve the PDEs of SFS [10, 11]. SFS is also formulated as viscosity solutions of static Hamilton–Jacobi (H–J) equations [12, 13]. There are mainly two classes of numerical methods for solving static H–J equations in SFS. The first class is based on reformulating the equations into suitable time-dependent problems. The heat equation of SFS [14] proposed recently belongs to this class. In the other class of numerical methods, the problem is treated as a stationary boundary value problem: it is discretized into a system of nonlinear equations. Such methods are the fast marching method [15], and level set method [16]. The merit of a viscosity solution theory in dealing with SFS is the following. Firstly, the ill-posed problem can be refined as a well-posed one. Secondly, reflectance models can be chosen flexibly, so SFS can be easily solved under both orthographic and perspective projection. The numerical methods of PDEs are consistent with digital characteristics of images.

Based on the viscosity solution theory, a new perspective SFS method is proposed in this paper. The reflectance map equation is formulated under perspective projection and turned into a static H–J equation. The SFS problem is a viscosity solution of the static H–J equation. Then, the fast iterative sweeping numerical method [17] is used to solve the H–J equation for its accuracy. Experiments presented in the fourth section show that the proposed shape reconstruction algorithm is more accurate than existing ones, such as the fast marching method [15]. The remainder of this paper is organized as follows. Section 2 introduces the reflectance model under perspective projection, and new H–J equations are derived. The fast sweeping numerical method and Gauss–Seidel iterations are discussed in the third section, and the flow chart of the proposed SFS algorithm is also given in this section. Experiments on both synthetic and real image are reported in Section 4. At last, conclusions are drawn in the fifth section.

## 2. Hamiltonian of perspective SFS

The brightness of image points mainly depends on four factors: the orientation of a light source, the location of a camera, the orientation of an object and the reflectance properties of the surface. SFS methods are based on satisfying the reflectance map (equation below) at each imaged point [2]

$$I(x, y) = R(x, y) \quad (1)$$

where  $I(x, y)$  and  $R(x, y)$  denote the image grey values and the reflectance map separately, and  $z = z(x, y)$  is the shape function to be reconstructed. Following,

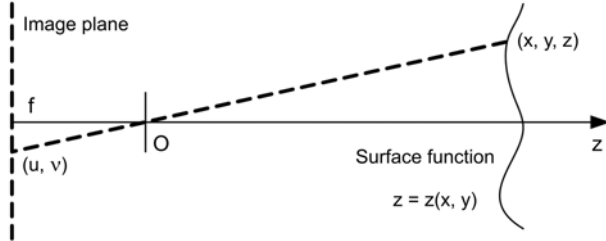


Fig. 1. Camera model using perspective projection.

$\mathbf{n}$  denotes the surface normal,  $\mathbf{s}$  is a light source vector. Two kinds of extreme reflection models, namely diffuse reflection and specular reflection, are usually considered in computer vision. In our SFS algorithm, the reflectance model is assumed to be a Lambertian (diffuse) reflectance model. When grey values of the image and the reflectance map are both normalized as  $E(x, y)$  and  $R(x, y)$ , the normalized reflectance map equation is described as

$$E(x, y) = \frac{I(x, y) - I_{\min}}{I_{\max} - I_{\min}} = R(x, y) = \frac{\mathbf{n} \cdot \mathbf{s}}{|\mathbf{n}| |\mathbf{s}|} \tag{2}$$

where  $I_{\max}$  and  $I_{\min}$  denote the maximum and minimum grey values of the captured image. Classical reflectance maps of SFS are mainly based on orthogonal projection. We will formulate the reflectance map (Eq. (2)) under perspective projection illustrated in Fig. 1.

In Figure 1, a scene surface  $S$  is defined as  $z = z(x, y)$ . An image pixel is denoted as  $(u, v)$  at the imaging plane  $z = -f$ , where  $f$  is the focal length. The perspective projection equation is  $x/u = y/v = -z/f$ . Thus, the surface  $S$  can be written as

$$S = \left( -\frac{fz}{u}, -\frac{fz}{v}, z(u, v) \right)$$

So the unit normal vector of the surface is given by [15] as

$$\mathbf{n} = \frac{(fz_u, fz_v, uz_u + vz_v + z)}{\sqrt{(uz_u + vz_v + z)^2 + f^2(z_u^2 + z_v^2)}} \tag{3}$$

where  $(z_u, z_v) = (\partial z / \partial u, \partial z / \partial v)$ , and  $\mathbf{s} = (-p_0, -q_0, 1)$  denotes the light source vector. When (3) is substituted into (2), we get the reflectance map under perspective projection in the imaging plane:

$$E(u, v) = \frac{(u - p_0 f)z_u + (v - q_0 f)z_v + z}{\sqrt{p_0^2 + q_0^2 + 1} \sqrt{(uz_u + vz_v + z)^2 + f^2(z_u^2 + z_v^2)}} \tag{4}$$

When we denote

$$(p, q) = \left( \frac{\partial \ln z}{\partial u}, \frac{\partial \ln z}{\partial v} \right) \quad (5)$$

and rearrange (4), we have

$$E(u, v) = \frac{(u - p_0 f)p + (v - q_0 f)q + 1}{\sqrt{p_0^2 + q_0^2 + 1} \sqrt{(up + vq + 1)^2 + f^2(p^2 + q^2)}} \quad (6)$$

Then, the corresponding H–J equation of SFS is

$$H(p, q, u, v) = E(u, v) \sqrt{(up + vq + 1)^2 + f^2(p^2 + q^2)} - \frac{(u - p_0 f)p + (v - q_0 f)q + 1}{\sqrt{p_0^2 + q_0^2 + 1}} \quad (7)$$

### 3. Fast sweeping algorithm for H–J equation of SFS

The fast sweeping method is based on the Lax–Friedrichs (L–F) monotone numerical Hamiltonians to approximate viscosity solutions of static H–J equations [17]. The Gauss–Seidel iteration and alternating sweeping scheme can be used in computation procedures in order to achieve the fast convergence. One of the merits of the fast sweeping method is that it can handle both convex and non-convex functions. The sweeping algorithms are fast since they do not require a sorting-heap structure required in the fast marching methods. We consider the following static H–J equation

$$\begin{cases} H(p, q, u, v) = 0 & (u, v) \in \frac{\Omega}{\Gamma} \\ z(u, v) = g(u, v) & (u, v) \in \Gamma \end{cases} \quad (8)$$

where  $\Omega$  is the image domain in  $R^2$ , and  $\Gamma$  is a subset (boundary) of  $\Omega$ . The Hamiltonian  $H$  is a nonlinear Lipschitz continuous function. Let us consider a uniform discretization:  $\{(u_i, v_j), i = 1, 2, \dots, M; j = 1, 2, \dots, N\}$  of  $\Omega$  with grid size  $(\Delta u, \Delta v)$ . The L–F Hamiltonian is

$$H(p^+, p^-, q^+, q^-) = H\left(\frac{p^+ + p^-}{2}, \frac{q^+ + q^-}{2}\right) - \left(\frac{p^+ - p^-}{2} \sigma_x + \frac{q^+ - q^-}{2} \sigma_y\right) \quad (9)$$

where  $p^\pm$  and  $q^\pm$  are corresponding forward and backward difference approximations of  $p$  and  $q$ , and  $\sigma_x$  and  $\sigma_y$  are artificial viscosities satisfying

$$\sigma_x \geq \max \left| \frac{\partial H}{\partial p} \right|, \quad \sigma_y \geq \max \left| \frac{\partial H}{\partial q} \right|$$

From (5), we denote  $Z_{i,j} = \ln z_{i,j}$  and

$$\begin{aligned} p_{i,j}^+ &= \frac{Z_{i+1,j} - Z_{i,j}}{\Delta u}, & p_{i,j}^- &= \frac{Z_{i,j} - Z_{i-1,j}}{\Delta u} \\ q_{i,j}^+ &= \frac{Z_{i,j+1} - Z_{i,j}}{\Delta v}, & q_{i,j}^- &= \frac{Z_{i,j} - Z_{i,j-1}}{\Delta v} \end{aligned} \quad (10)$$

When (10) is substituted into (9), and rearranged as

$$\begin{aligned} Z_{i,j} &= -\frac{1}{\frac{\sigma_x}{\Delta u} + \frac{\sigma_y}{\Delta v}} \left[ -H \left( \frac{Z_{i+1,j} - Z_{i-1,j}}{2\Delta u}, \frac{Z_{i,j+1} - Z_{i,j-1}}{2\Delta v} \right) + \right. \\ &\quad \left. + \left( \sigma_x \frac{Z_{i+1,j} + Z_{i-1,j}}{2\Delta u} + \sigma_y \frac{Z_{i,j+1} + Z_{i,j-1}}{2\Delta v} \right) \right] \end{aligned}$$

So, the iterative formula is

$$\begin{aligned} Z_{i,j}^{(k+1)} &= -\frac{1}{\frac{\sigma_x}{\Delta u} + \frac{\sigma_y}{\Delta v}} \left[ -H \left( \frac{Z_{i+1,j} - Z_{i-1,j}}{2\Delta u}, \frac{Z_{i,j+1} - Z_{i,j-1}}{2\Delta v} \right) + \right. \\ &\quad \left. + \left( \sigma_x \frac{Z_{i+1,j} + Z_{i-1,j}}{2\Delta u} + \sigma_y \frac{Z_{i,j+1} + Z_{i,j-1}}{2\Delta v} \right) \right] \end{aligned} \quad (11)$$

where  $k$  is an iteration step. There is no superscript in the right part of (11) because these superscripts are determined by sweeping directions of Gauss–Seidel iterations.

The fast sweeping method consists in applying upwind difference formulae, and is based on Gauss–Seidel iterations to update unknown function values. The sweeping direction should ideally correspond to the real direction of information propagation. There are four different sweeping directions in SFS: *i*) from lower left to upper right; *ii*) from lower right to upper left; *iii*) from upper left to lower right; and *iv*) from upper right to lower left. If sweeping is from left-down to right-up, then  $Z_{i-1,j} = Z_{i-1,j}^{(k+1)}$ ,  $Z_{i,j-1} = Z_{i,j-1}^{(k+1)}$ ,  $Z_{i+1,j} = Z_{i+1,j}^{(k)}$ ,  $Z_{i,j+1} = Z_{i,j+1}^{(k)}$  because the newest values are used in the Gauss–Seidel iteration. Other situations are similar when we deal with other three sweeping directions using the Gauss–Seidel iteration.

There are mainly three steps: initialization, alternating sweeping, and enforcing computational boundary conditions during the iterative procedures of computing (11). Consider a uniform discretization of  $\{(u_i, v_j), i = 1, 2, \dots, M; j = 1, 2, \dots, N\}$  of imaging the domain denoted as  $\Omega$  with the pixel size  $\Delta u = \Delta v$ , where the resolution of the image is  $M \times N$ . The new fast sweeping algorithm of SFS is summarized as follows.

*Initialization:* Fix exact values on the boundary of the domain, and extrapolate values near the boundary according to boundary conditions. These values are not changed during the iterations. For other pixel points, a large positive value  $C$  is assigned, where  $C$  should be larger than the maximum of the solutions, and these values will be renewed during the process of iterations.

*Alternating sweeping iteration:* At iteration  $(k + 1)$ ,  $Z_{i,j}^{(k+1)}$  are calculated according to (11) at all pixel points  $\{(u_i, v_j)\}$  except for those with fixed values. And  $Z_{i,j}$  is updated only when  $Z_{i,j}^{(k+1)}$  is less than the previous value  $Z_{i,j}^{(k)}$ . This process changes four different directions alternatively, as discussed above, namely *i*)  $i = 1:M, j = 1:N$ ; *ii*)  $i = M:1, j = 1:N$ ; *iii*)  $i = 1:M, j = N:1$ ; and *iv*)  $i = M:1, j = N:1$ .

*Renewing boundary values:* On the boundary, a set of conditions should be imposed, suggested in [17] as

$$\begin{cases} Z_{0,j}^{(k+1)} = \min\left(\max(Z_{1,j} - Z_{2,j}), Z_{0,j}^{(k)}\right) \\ Z_{M,j}^{(k+1)} = \min\left(\max(Z_{M-1,j} - Z_{M-2,j}), Z_{M,j}^{(k)}\right) \\ Z_{i,0}^{(k+1)} = \min\left(\max(Z_{i,1} - Z_{i,2}), Z_{i,0}^{(k)}\right) \\ Z_{i,N}^{(k+1)} = \min\left(\max(Z_{i,N-1}^{(k+1)} - Z_{i,N-2}^{(k+1)}), Z_{i,N}^{(k)}\right) \end{cases} \quad (12)$$

If the boundary is not rectangle, similar computation is also valid. Linear extrapolation is also an alternative choice [17].

*Stop criteria:* If  $|Z_{i,j}^{(k+1)} - Z_{i,j}^{(k)}| \leq \delta$ , where  $\delta$  is a given positive threshold value, the computation stops.

#### 4. Experimental results

To evaluate the performance of the proposed SFS method, we have done series of comparing experiments with fast marching SFS methods proposed recently [15]. The fast marching method is fast and effective according to reference [15]. Small iterative times are required in the fast marching method. And both orthographic and perspective projection can be dealt with. Experiments on both synthetic and real images are performed. Reconstructed 3-D shapes from synthetic images are shown and numerically compared with the real shape to illustrate the accuracy of the reconstruction methods. Reconstruction results from real images are also given and new numerical comparing criteria using a reflectance map are also proposed. All the algorithms are realized under the following conditions: hardware – CPU-AMD 1.7 GHZ, RAM-256MB; software – Windows 2000 and Matlab 6.5.

### 4.1. Experiments with the synthetic image of a vase

The original 3-D shape and synthetic image of a vase (13) [3] generated mathematically by equation (6) are shown in Figs. 2a and 2b.

$$z(u, v) = \sqrt{\left[0.15 - 0.1v(6v + 1)^2(v - 1)^2(3v - 2)\right]^2 - u^2}, \quad 0 \leq |u| \leq 0.5, \quad 0 \leq v \leq 1 \quad (13)$$

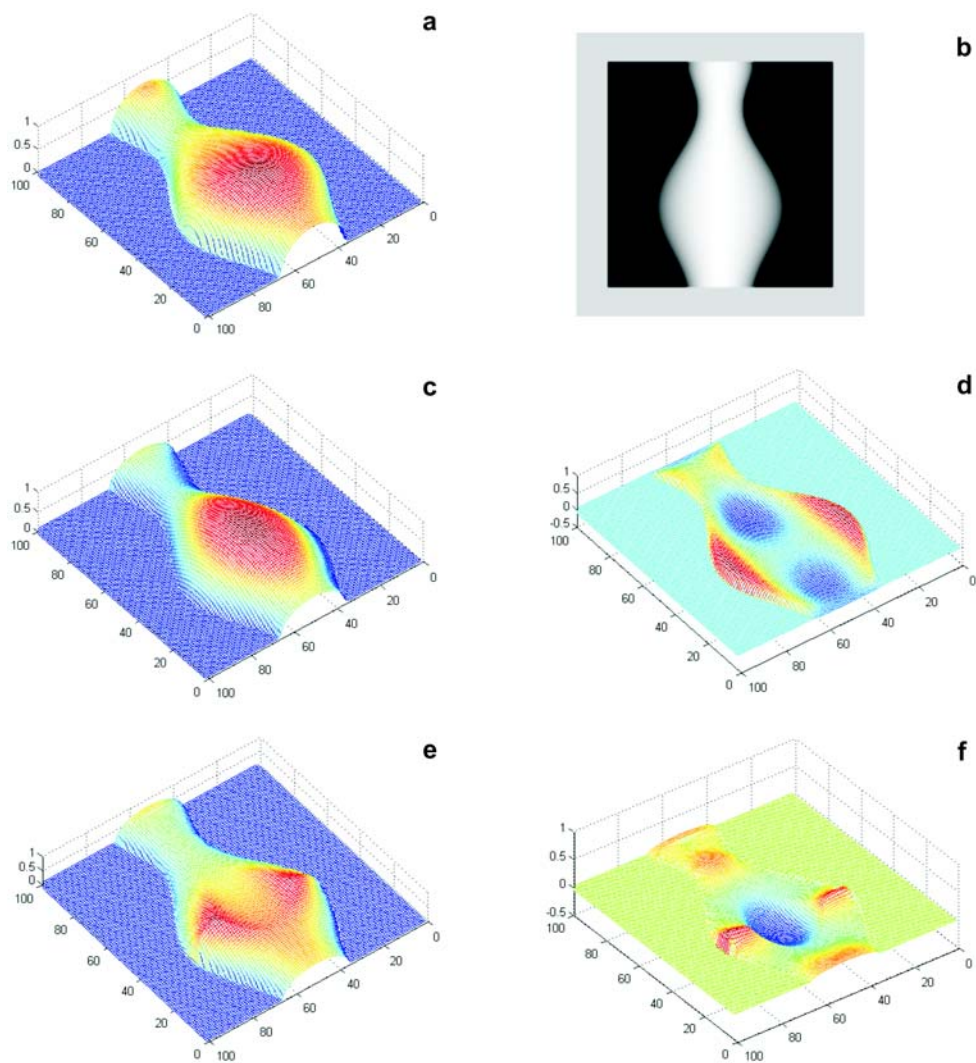


Fig. 2. Reconstructed 3-D shape of a synthetic vase: the original shape of a vase (a), the synthetic image of a vase (b), reconstructed shape by the proposed method (c), the deviation of fig. c from a (d), reconstructed shape by Tankus [15] (e), the deviation of fig. e from a (f).

Table 1. The comparison of numerical results of the proposed method with Tankus' method [15] of a synthetic vase.

Iterations	The proposed method			Tankus' method		
	ME (pex)	RS (pex)	$T$ (sec)	ME (pex)	RS (pex)	$T$ (sec)
1	0.0934	0.1698	1.0565	0.2213	0.3840	1.2020
5	0.0555	0.1122	5.4375	0.0248	0.0563	6.2340
10	0.0389	0.0788	10.8255	0.0324	0.0784	13.0185
15	0.0304	0.0620	16.2685	0.0392	0.0881	19.3225
20	0.0274	0.0560	21.7615	0.0396	0.0885	25.5265
25	0.0278	0.0564	25.3260	0.0397	0.0885	32.2610
30	0.0272	0.0559	31.9210	0.0396	0.0885	40.4710

The direction of light and the focus length  $f$  in Eq. (6) are  $(0,0,1)$  and 100, respectively. Pixels of the image are  $100 \times 100$ . The synthetic image is produced by multiplying values of the normalized reflectance map with imaging coefficient 255. The surface reconstructed using the proposed method is shown in Fig. 2c after 30 iterations. Figure 2d shows the deviation of the 3-D shape reconstructed using the proposed method from the original surface. In Figures 2e and 2f there are reconstructed shapes obtained using the method of Tankus [15] and the deviation of the 3-D reconstructed shape from the original surface after the same number of iterations. The unit in figures is a pixel. In our experiments, the height of the reconstructed 3-D surface was normalized after each iteration due to an interesting characteristic shown as Eq. (5) in perspective SFS. The surfaces  $z(u, v)$  and  $Kz(u, v)$  have the same reflectance map function, where  $K$  is some non-zero positive constant.

Table 1 contains the numerical results compared with the original shape of a vase illuminated as in Fig. 2. In Table 1 there are presented such criteria as the mean error (ME), the root squares mean error (RS) of the reconstructed shape compared with the original shape, and cpu times  $T$ , which are used to compare the performances of two SFS methods.

From the comparison of results illustrated by Fig. 2 and Tab. 1, we can see that the proposed fast sweeping method is more effective than the fast marching method of [15]. The main drawback of the fast marching method of [15] is that the depths of local minimal or maximal points should be given before iterative computation. Otherwise a distortion of a reconstructed shape may occur. In our experiments, because we only want to compare the performance of the proposed method with the fast marching method, the depths of local minimal or maximal points are not pointed. So in the reconstruction results shown in Fig. 2e an obvious distortion around the top of the vase occurs. Table 1 shows that both methods can give a stable resolution after 15 iterations. The fast marching method is more accurate than the proposed method at first several iterations. But the final stable reconstructed shape of the proposed method

has smaller mean error (ME) and root squares mean error (RS) than the fast marching method. The numerical error in both methods may be produced by discrete sampling of imaging and discrete difference approximating. Table 1 also shows that the proposed method is slightly faster than the fast marching method.

#### 4.2. Experiments with real image

Figure 3a shows a real image of metal statuary of Qian WueSeng captured by us in Xi'an Jiaotong University using Cannon digital camera after mean filtering. A focus length  $f$  is 40 mm. Pixels of images are  $320 \times 280$ . Because the width of the statuary is about 40 cm, the focus length  $f$  is 28 pixels in image coordinates. Because the flash light of the camera is the light source, the direction of light is  $(0,0,1)$  approximately. Figure 3b is the reconstructed shape obtained using the proposed method after 30 iterations. Figure 3c is the reconstructed image obtained using the reflectance map equation (6) calculated from the computed surface using the proposed method. Figure 3d is the reconstructed shape obtained using the method of Tankus [15] after the same number of iterations. Figure 3e is the corresponding reconstructed image obtained using the same reflectance map equation calculated from the computed surface using the method of Tankus [15].

In this experiment, the real surface of metal statuary was difficult to measure. So we compared numerically the pixel values of the images reconstructed using the reflectance map equation (6) with the pixel values of the original image. Table 2 presents the numerical result of the pixel values of the reconstructed images using two methods compared with the original image of the statuary illuminated in Fig. 3a. In Table 2, the criteria such as mean error (ME) of the pixel values of the reconstructed images compared with the original image, root squares mean error (RS) of the pixel values of the reconstructed images compared with the original image and cpu times  $T$  were used to compare the performances of two SFS methods. The units of ME and RS are 8bit (256) grey-level, and the unit of cpu times is second.

After comparing the results illustrated by Fig. 3 and Tab. 2, we can see that the proposed method is more accurate than the fast marching method of [15]. In this experiment, because the boundary conditions are not known, we assumed zero boundary conditions in both reconstruction methods. But both methods are sensitive to the boundary conditions. So the presence of an error in the reconstructed 3-D shape is obvious. And for the fast marching method, because the depths of local minimal or maximal points are unknown, there exists a great distortion in the reconstructed 3-D shape shown in Fig. 3d. The reconstructed 3-D shape of the proposed method shown in Fig. 3b is more vivid than in Fig. 3d. The reconstructed images obtained using the reflectance map equation (6) calculated from the reconstructed surface using the proposed method and Tankus's method shown in Figs. 3c and 3e, illustrate intuitively that the proposed method is more effective than Tankus's. Furthermore, the comparison of numerical results of the reconstructed images with the original

image of the metal statuary shown in Tab. 2 confirms the intuition of Fig. 3. As in the first experiment, Tankus's method converged quickly at first 20 iterations. But the proposed method exceeded Tankus's method when they tended to stable solution.

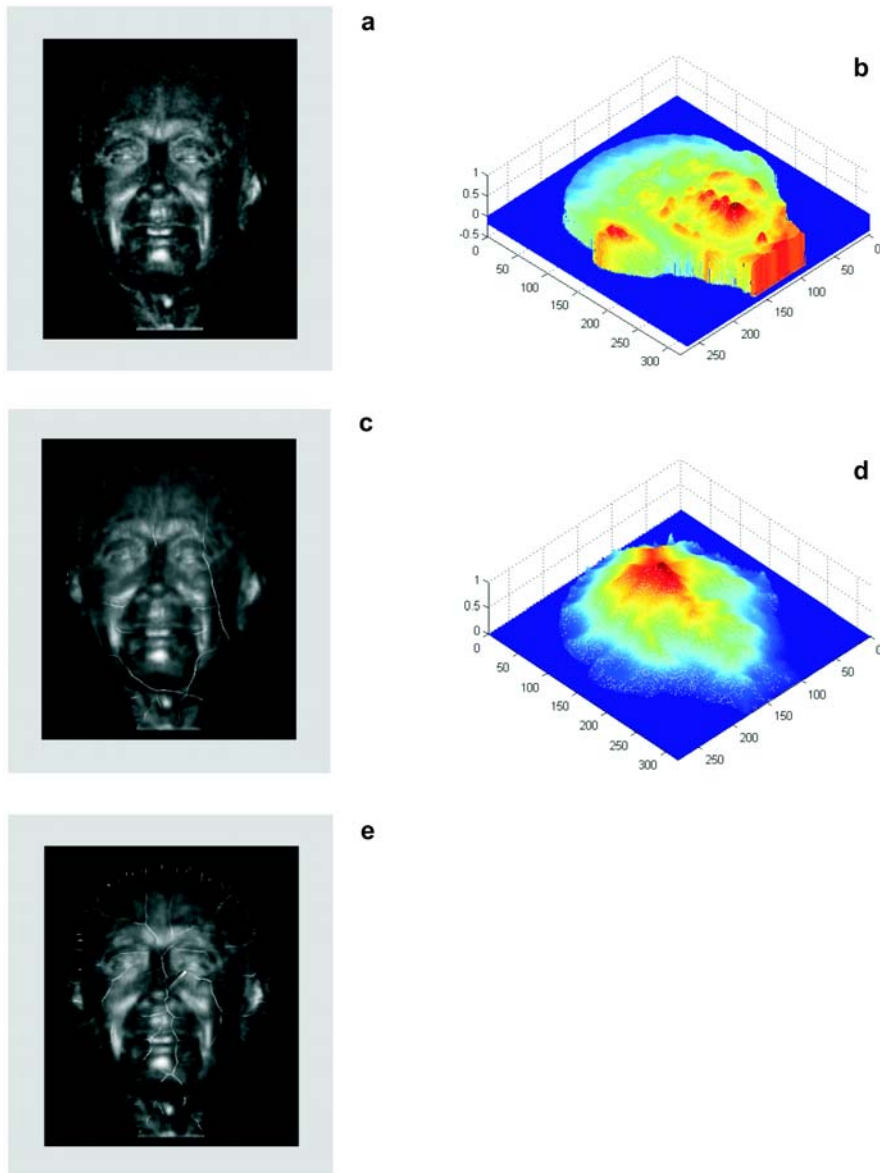


Fig. 3. Reconstructed shape of metal statuary of Qian WueSeng: captured image after mean filtering (a); reconstructed shape obtained using the proposed method (b); reconstructed image obtained using the reflectance map calculated from the computed surface using the proposed method (c); reconstructed shape obtained using the method of Tankus [15] (d); reconstructed image obtained using the reflectance map calculated from the computed surface using the method of Tankus [15] (e).

T a b l e 2. Comparison of numerical results of reconstructed images with the original image of a metal statuary.

Iterations	The proposed method			Tankus' method		
	ME (grey)	RS (grey)	$T$ (sec)	ME (grey)	RS (grey)	$T$ (sec)
1	32.1977	53.2247	41.0940	12.4126	26.9340	54.1560
5	40.303	68.5836	202.186	13.9164	30.1053	280.624
10	20.9485	42.8400	401.658	13.0244	28.3864	548.124
15	14.1671	31.0477	601.158	10.7110	24.7376	819.468
20	10.4983	21.7074	807.220	9.4584	22.5164	1094.50
25	7.7088	16.9490	1013.00	8.1655	20.4552	1371.10
30	6.0667	13.7159	1216.70	6.2870	15.9434	1649.40

We also see that the proposed method is faster than the compared method per iteration. Besides the numerical error, in both methods produced by discrete sampling of imaging and discrete difference approximating, the imaging model error is inevitable. Highlight, namely the specular reflectance of an acquired image should be included into the reflectance model for metal surfaces. But investigators seldom considered this problem. This may be the subject of our further study.

## 5. Conclusions

In this paper, a new perspective SFS method is proposed. Using the conception of viscosity solution of static H–J equation and fast sweeping numerical scheme, the SFS problem under perspective projection is solved. The experiments are performed both on synthetic and real images. As for synthetic images, numeric comparing criteria such as mean error and root squares mean error of reconstructed 3-D shape with original surface and cpu times  $T$  were used to evaluate the performance of the proposed method. As for real images, new numeric comparing criteria such as mean error and root squares mean error of pixel values of reconstructed 2-D images with pixel values of the original images were proposed. Experiments on synthetic images and real images show that the proposed SFS is fast and accurate and may be used to deal with complicated surfaces. Shape from shading under perspective projection is one of main directions of SFS. How to formulate the reflectance map equation using more suitable reflectance models under this kind of projection framework is an interesting issue. We are also investigating how to deal with boundary conditions of viscosity solution of static Hamilton–Jacobi systems in SFS.

## Reference

- [1] HORN B.K.P., *Height and gradient from shading*, International Journal of Computer Vision **5**(1), 1990, pp. 37–75.
- [2] ZHANG R., TSAI P.S., CRYER J.E., SHAH M., *Shape from shading: a survey*, IEEE Transactions on Pattern Analysis and Machine Intelligence **21**(8), 1999, pp. 690–706.

- [3] CHO S.Y., CHOW T.W.S., *A new color 3D SFS methodology using neural-based color reflectance models and iterative recursive method*, Neural Computation **14**(11), 2002, pp. 2751–89.
- [4] DU Q.Y., BEN S.C., LIN T., *An application of shape from shading*, 8th International Conference on Control, Automation, Robotics and Vision, Vol. 1, 2004, pp. 184–9.
- [5] RAJABI M.A., BLAIS J.A.R., *Optimization of DTM interpolation using SFS with single satellite imagery*, The Journal of Supercomputing **28**(2), 2004, pp. 193–213.
- [6] BORS A.G., HANCOCK E.R., WILSON R.C., *Terrain analysis using radar shape-from-shading*, IEEE Transactions on Pattern Analysis and Machine Intelligence **25**(8), 2003, pp. 974–92.
- [7] JIANG T., LIU B., LU Y.L., EVANS D.J., *A neural network approach to shape from shading*, International Journal of Computer Mathematics **80**(4), 2003, pp. 433–9.
- [8] CROUZIL A., DESCOMBES X., DUROU J.D., *A multiresolution approach for shape from shading coupling deterministic and stochastic optimization*, IEEE Transactions on Pattern Analysis and Machine Intelligence **25**(11), 2003, pp. 1416–21.
- [9] LIN C.T., CHENG W.C., LIANG S.F., *Neural-network-based adaptive hybrid-reflectance model for 3-D surface reconstruction*, IEEE Transactions on Neural Networks **16**(6), 2005, pp. 1601–15.
- [10] ROUY E., TOURIN A., *A viscosity solutions approach to shape-from-shading*, SIAM Journal on Numerical Analysis **29**(3), 1992, pp. 867–84.
- [11] PRADOS E., *Application of the theory of the viscosity solutions to the shape from shading problem*, PhD Thesis, University of Nice-Sophia Antipolis, France 2004.
- [12] LIONS P.L., ROUY E., TOURIN A., *Shape-from-shading, viscosity solutions and edges*, Numerische Mathematik **64**(3), 1993, pp. 323–53.
- [13] KIMMEL R., BRUCKSTEIN A., *Global shape from shading*, Computer Vision and Image Understanding **62**(3), 1995, pp. 360–9.
- [14] ROBLES KELLY A., HANCOCK E.R., *Shape-from-shading using the heat equation*, IEEE Transactions on Image Processing **16**(1), 2007, pp. 7–21.
- [15] TANKUS A., SOCHEN N., YESHURUN Y., *Shape-from-shading under perspective projection*, International Journal of Computer Vision **63**(1), 2005, pp. 21–43.
- [16] KIMMEL R., BRUCKSTEIN A.M., *Tracking level sets by level sets: A method for solving the shape from shading problem*, Computer Vision and Image Understanding **62**(1), 1995, pp. 47–58.
- [17] KAO C.Y., OSHER S., QIAN J., *Lax–Friedrichs sweeping scheme for static Hamilton–Jacobi equations*, Journal of Computational Physics **196**(1), 2004, pp. 367–91.

*Received November 8, 2007  
in revised form February 26, 2008*